Proof Delivery Form

Journal and Article number: BJ2014-1550

BJ reference: BJ2014/1550

Number of colour figures: Figures 1, 2, 3, 4, 5, and 7

FOR PUBLISHER'S USE ONLY

Article Type _____

Pages with colour figs (main article)_____

Supplementary online data?

PDF _____

Animation _____

3D Interactive Structure _____

Movie _____

Other _____

Commentary

BJ20____/_____

Figures/schemes/tables to be replaced

Main article figure _____

Main article scheme _____

Main article table _____

New text _____

Revised proof to author? _____

Other comments

Number of pages (not including this page): 14

Biochemical Journal

Please check your proof carefully to ensure (a) accuracy of the content and (b) that no errors have been introduced during the production process.

- You are responsible for ensuring that any errors contained in this proof are marked for correction before publication. Errors not marked may appear in the published paper.
- Corrections should only be for typographical errors in the text or errors in the artwork; substantial revision of the substance of the text is not permitted.
- Please answer any queries listed below.
- If corrections are required to a figure, please supply a new copy.

Your proof corrections and query answers should be returned as soon as possible (ideally within 48 hours of receipt). You can send proofs by email (editorial@portlandpress.com) or fax (+44 (0)20 7685 2469). Corrections sent by email can be sent as attachments, i.e. annotated PDF files or scanned versions of marked-up proofs

Notes:

1. Please provide the paper's reference number in any correspondence about your article
2. If you have any queries, please contact the publisher by email (editorial@portlandpress.com) or by telephone +44 (0)20 7685 2410

Supplementary Material:

This proof does not contain any supplementary material. If supplementary content is associated with this article it will be published, in the format supplied by the authors, with the online version of the article.

Summary Statement (please check):

Sialidase NEU3 is a key enzyme in the catabolism of gangliosides. We demonstrated that NEU3 impairs cargo internalization via clathrin-coated pits, affecting AP-2 subcellular distribution. This study delineates previously unidentified cellular functions of NEU3.

Please return this form with your proof

Queries for author:

Q1: Please provide the force in $\boldsymbol{g}$.
Q2: If grant numbers are available, please include them within square brackets after each funding body.

Notes to Publisher:

Non-printed material (for Publisher's use only):

Primary: S2

Please return this form with your proof

Order for Offprints for the *Biochemical Journal*

Article number **BIC**..... No. of pages .....

Reference number **BJ20**..... / ..... Title of paper .....

.....

SECTION 1– INFORMATION

Please return this form with your proof to: *Biochemical Journal* Editorial Office, FAX: +44 (0)20 7685 2469
(Portland Press Limited, Third Floor, Charles Darwin House, 12 Roger Street, London WC1N 2JU, UK).

Offprints must be ordered using this form. If an official order form from your organization is required, it may be sent on later (please quote the article and reference numbers above), but it will be assumed that any such order received is not an additional order. Free offprints are not available and offprints cannot be supplied after publication.

Offprint orders are despatched by surface mail approximately 2 weeks after publication (allow up to 6 months for delivery). If you wish them to be despatched by Airmail please tick the box in section 2 below and add 40% to the indicated price.

If your article contains supplementary online data, please note that any offprints ordered will not include this material.

***Biochemical Journal* 2011 Offprint Order Charges**

Number of pages	Number required [price in Pounds sterling (£)]					
	50	**100**	**200**	**300**	**400**	**500**
1–4	150	198	313	427	531	630
5–8	198	265	427	588	735	884
9–12	262	346	575	805	1012	1218
13–16	320	427	749	1068	1369	1667

Notes

1. For quantities not listed, please ask for a quotation
2. Prices revised October 2007. No price increase in 2011.

SECTION 2– ORDER

☐ I do not wish to order offprints of my article

☐ I wish to purchase..... (minimum 50) offprints of my article at a cost of ..... £/$/€

☐ Please send my offprints by Airmail (add 40% to the price indicated) at an additional cost of ..... £/$/€

☐ Bank charges (if applicable, see section 3) ..... £/$/€

Total cost ..... £/$/€

Name and address to which offprints should be sent (please enter this information clearly):

.....

.....

.....

.....

.....

SECTION 3– PAYMENT

We accept payment:

- in pound sterling cheques drawn on UK banks
- in US dollar cheques drawn on US banks
- in Euro cheques drawn on any European bank
- by Visa, Mastercard and most major debit cards

For payment in $US or Euros, please convert the price shown above at the current rate of exchange and add £15 for bank charges.

Please indicate your preferred payment option:

1 ☐ I enclose a remittance payable to Portland Press Limited

2 ☐ Please send an invoice to the following address (if different from address in section 2)

.....

.....

.....

.....

.....

3 ☐ I wish to pay by Visa/Mastercard/Visa Delta/Switch/ Maestro (delete as appropriate)

Card number: .....

Name on card: .....

Start date ..... End date .....

Issue no (Switch only): .....

Full address of cardholder:

.....

.....

.....

.....

Cardholder signature ..... Date.....

Biochemical Journal Editorial Office, Portland Press Limited, Third Floor, Charles Darwin House, 12 Roger Street, London WC1N 2JU, UK
Tel: +44 (0)20 7685 2410; fax: +44 (0)20 7685 2469; email: editorial@portlandpress.com; WWW: http://www.portlandpress.com

portlandpresslimited
publishing innovation

Role of plasma-membrane-bound sialidase NEU3 in clathrin-mediated endocytosis

Macarena Rodriguez-Walker*[1], Aldo A. Vilcaes*[1], Eduardo Garbarino-Pico* and José L. Daniotti*[2]

*Centro de Investigaciones en Química Biológica de Córdoba (CIQUIBIC, UNC-CONICET), Departamento de Química Biológica, Facultad de Ciencias Químicas, Universidad Nacional de Córdoba, Córdoba, Argentina

Gangliosides are sialic acid-containing glycosphingolipids mainly expressed at the outer leaflet of the plasma membrane. Sialidase NEU3 is a key enzyme in the catabolism of gangliosides with its up-regulation having been observed in human cancer cells. In the case of CME (clathrin-mediated endocytosis), although this has been widely studied, the role of NEU3 and gangliosides in this cellular process has not yet been established. In the present study, we found an increased internalization of Tf (transferrin), the archetypical cargo for CME, in cells expressing complex gangliosides with high levels of sialylation. The ectopic expression of NEU3 led to a drastic decrease in Tf endocytosis, suggesting the participation of gangliosides in this process. However, the reduction in Tf endocytosis caused by NEU3 was still observed in glycosphingolipid-depleted cells, indicating that NEU3 could operate in a way that is independent of its action on gangliosides. Additionally, internalization of α_2-macroglobulin and low-density lipoprotein, other typical ligands in CME, was also decreased in NEU3-expressing cells. In contrast, internalization of cholera toxin β-subunit, which is endocytosed by both clathrin-dependent and clathrin-independent mechanisms, remained unaltered. Kinetic assays revealed that NEU3 caused a reduction in the sorting of endocytosed Tf to early and recycling endosomes, with the Tf binding at the cell surface being also reduced. NEU3-expressing cells showed an altered subcellular distribution of clathrin adaptor AP-2 (adaptor protein 2), but did not reveal any changes in the membrane distribution of clathrin, PtdIns(4,5)P_2 or caveolin-1. Overall, these results suggest a specific and novel role of NEU3 in CME.

Key words: clathrin, ganglioside, glycolipid, membrane trafficking, NEU3, sialidase.

INTRODUCTION

Endocytosis is an essential process for diverse cellular functions such as nutrient uptake, cell communication, plasma membrane remodelling and internalization of lipids and receptor-bound macromolecules [1,2]. Several entry pathways into cells have been identified, which vary in the cargoes that they transport and in the protein and lipid machinery that facilitate the endocytic process.

CME (clathrin-mediated endocytosis) constitutes the principal and best characterized route for selective receptor internalization in higher eukaryotic cells [3]. More recently, however, several endocytic pathways that do not use clathrin have also been reported. These pathways, constitutive or triggered by specific signals, often differ in their mechanism of formation, molecular machinery and cargo destination [4–7].

Gangliosides, which are sialylated glycosphingolipids, are key signalling molecules in biological events that have been implicated in many physiological processes, including growth, signalling, migration, membrane trafficking and apoptosis. Moreover, some ganglioside functions are undesirable, as they are receptors for viruses, toxins and antibodies [8–10]. Gangliosides are typically anchored in the outer leaflet of the plasma membrane and are widely found in vertebrate tissues. Their *de novo* synthesis starts at the endoplasmic reticulum and is continued by a combination of glycosyltransferase activities at the Golgi complex, followed by vesicular delivery to the plasma membrane [11,12]. At the cell surface, gangliosides can undergo endocytosis, and, once internalized, they can be sorted into endosomes or degraded by glycohydrolases at the lysosomal level. Recently, a number of enzymes for ganglioside anabolism and catabolism have been shown to be associated with the plasma membrane, which were able to exert their enzymatic activities on substrates belonging to the surface of both their own and neighbouring cells [13–16]. It has been hypothesized, and in some cases clearly demonstrated, that these activities are responsible for the fine-tuning of the plasma membrane ganglioside composition, and, consequently, the functional properties of plasma membrane proteins involved in different signalling processes [17,18].

Sialidases are glycohydrolases that catalyse the removal of α-glycosidically linked sialic acid residues from carbohydrate groups of glycoproteins and glycolipids. Four types of mammalian sialidases have been identified and characterized to date, which have been designated NEU1, NEU2, NEU3 and NEU4. They are encoded by different genes and differ in their major subcellular localization and enzymatic properties. In particular, NEU3 is mainly expressed at the plasma membrane and is a key enzyme in the catabolism of membrane gangliosides. For this reason, NEU3 has been implicated in processes similar to those involving gangliosides, such as adhesion, differentiation, cancer progression and apoptosis [17,19–21]. A remarkable up-regulation (3–100-fold) of NEU3 has been observed in various human cancer cells, in which a high concentration of the enzyme regulates

Abbreviations: α_2M, α_2-macroglobulin; α_2M–Alexa^{594}, Alexa Fluor® 594-conjugated α_2M; AP-2, adaptor protein 2; β3GalT-IV, β-1,3-galactosyltransferase; β4GalNAcT-I, β-1,4-*N*-acetylgalactosaminyltransferase; CHO, Chinese-hamster ovary; CLC, clathrin light chain; CME, clathrin-mediated endocytosis; CTx, cholera toxin; CTxβ, CTx β-subunit; CTxβ–Alexa^{555}, Alexa Fluor® 555-conjugated CTxβ; DMEM, Dulbecco's modified Eagle medium; HPTLC, high-performance TLC; LAMP1, lysosome-associated membrane protein 1; LDL, low-density lipoprotein; PH, pleckstrin homology; PLCδ1, phospholipase Cδ1; qPCR, quantitative real-time PCR; Tf, transferrin; Tf–Alexa^{647}, Alexa Fluor® 647-conjugated human Tf; TfR, Tf receptor.

[1] These authors contributed equally to this work.

[2] To whom correspondence should be addressed (email daniotti@dqb.fcq.unc.edu.ar).

transmembrane signalling at the plasma membrane, through both the modulation of ganglioside expression and by direct interaction with signal molecules such as epidermal growth factor receptor [22,23]. In addition, NEU3 has been described to be closely associated with caveolin-1 in membrane microdomains [24] with its silencing enhancing the caveolar endocytosis of β1 integrin, blocking its recycling and reducing its levels at the cell surface [25]. On the other hand, while we were examining endocytosis in a panel of cell lines genetically modified to express different ganglioside species, we observed that expression of complex and highly sialylated gangliosides correlates with an increased internalization of cargoes via CME. Thus, to investigate further the participation of gangliosides in endocytic processes, we decided to study the consequences of their desialylation, by expression of the sialidase NEU3. Our results show that: (i) the ectopic expression of human NEU3 led to a drastic decrease in the CME of Tf (transferrin), LDL (low-density lipoprotein) and α_2M (α_2-macroglobulin); (ii) the up-expression of NEU3 did not modify the clathrin-independent endocytosis of CTx (cholera toxin); (iii) most of the effect of NEU3 on the Tf internalization is independent of its catabolic activity towards gangliosides; and (iv) the effect produced by NEU3 on CME involved an abnormal distribution of the clathrin adaptor AP-2 (adaptor protein 2), whereas the intracellular distribution of clathrin, PtdIns(4,5)P_2 and caveolin-1 remained unchanged. Overall, these results suggest a specific and novel role of NEU3 in CME and indicate that the sialidase might play crucial roles in regulation of cell-surface functions besides ganglioside catabolism.

EXPERIMENTAL

Expression plasmids

The constructs containing the DNA-coding sequence for human NEU3 tagged at the C-terminus with the epitope c-Myc were obtained by subcloning the corresponding full-length cDNA fragment into the pCI-neo (Promega) or pTracer-CMV (Invitrogen) mammalian expression vectors. Expression plasmids for wild-type GTPase Rab11a–GFP, wild-type GTPase Rab5–GFP, LAMP1 (lysosome-associated membrane protein 1)–GFP and glycosyltransferase β4GalNAcT-I–Cherry have been described elsewhere [26–28]. Plasmids coding for AP-2 σ2–GFP and CLC (clathrin light chain)–EYFP were generously supplied by J. Bonifacino (NICHD, National Institutes of Health, Bethesda, MD, U.S.A.) [29]. Plasmid PH-PLCδ1–RFP encoding the PH (pleckstrin homology) domain of PLCδ1 (phospholipase Cδ1) fused to RFP was kindly supplied by S. Grinstein (Department of Cell Biology, The Hospital for Sick Children, Toronto, ON, Canada).

Cell lines and cell cultures

The following cells were used: wild-type CHO (Chinese-hamster ovary)-K1 cells (CHO-K1^{GM3+}) (A.T.C.C., Manassas, VA, U.S.A.); CHO-K1 clone 2 (CHO-K1^{GD3+}), a stable chick CMP-NeuAc: GM3 sialyltransferase (ST8Sia-I, also called Sial-T2) transfectant expressing the gangliosides GD3 and GT3 [30]; CHO-K1 clone 4 (CHO-K1^{GD1a+}), a stable double transfectant expressing UDP-GalNAc:LacCer/GM3/GD3/GT3 β-1,4-*N*-acetylgalactosaminyltransferase (β4GalNAcT-I, also called GalNAc-T) and UDP-Gal:GA2/GM2/GD2 β-1,3-galactosyltransferase (β3GalT-IV, also called Gal-T2) [30] and having an increased expression of GM1 and GD1a; and COS-7 cells. Cells were grown and maintained at 37 °C in 5 % CO_2 in DMEM (Dulbecco's modified Eagle medium; Invitrogen) supplemented with 10 % (v/v) FBS and antibiotics. Transfections were carried out with 1 μg per 35-mm-diameter dish of the indicated plasmid using cationic liposomes (Lipofectamine; Invitrogen) or PEI (polyethyleneimine) (Sigma–Aldrich). CHO-K1^{GM3+}, CHO-K1^{GD3+} and CHO-K1^{GD1a+} cells transiently transfected with pCI-neoNEU3 are referred to as CHO-K1$^{GM3+,NEU3+}$, CHO-K1$^{GD3+,NEU3+}$ and CHO-K1$^{GD1a+,NEU3+}$ cells respectively. CHO-K1^{GM3+} cells transiently transfected with pTracerNEU3 (which expresses NEU3 and GFP under independent promoters) are referred to as CHO-K1$^{GM3+,GFP(NEU3)+}$ cells, with GFP expression being used as a marker to identify NEU3-expressing cells. Clones with stable expression of CLC–EYFP or AP-2 σ2–GFP were generated in CHO-K1^{GM3+} cells.

To generate stably NEU3-expressing cells, CHO-K1^{GM3+} cells were transfected with pTracerNEU3. Then, cells were sorted according to their GFP expression using a FACS CantoII cytometer (BD Biosciences) and cells with higher expression of GFP were collected. Stably transfected cells were selected by the addition of Zeocin™ (Invitrogen) as a selection marker. This mixed population of antibiotic-resistant cells was checked for NEU3 expression and used directly for experimental analysis.

Antibodies

The following antibodies were used: monoclonal mouse antibody against human NEU3 (MBL International Corporation), monoclonal and polyclonal antibodies against c-Myc produced in mouse and rabbit respectively (Sigma–Aldrich), polyclonal rabbit antibody against caveolin-1 (Abcam), monoclonal mouse antibody against GD3 (clone R24; A.T.C.C.), monoclonal mouse antibody against GD1a (kindly supplied by P.H. Lopez, INIMEC-CONICET, Córdoba, Argentina), monoclonal mouse antibody against tubulin (Sigma–Aldrich) and monoclonal mouse antibody against GFP (Roche). The secondary antibodies used were Alexa Fluor® 488-conjugated goat anti-mouse IgG, Alexa Fluor® 546-conjugated goat anti-mouse IgG, Alexa Fluor® 568-conjugated goat anti-mouse IgG, Alexa Fluor® 546-conjugated goat anti-rabbit IgG (Molecular Probes/Invitrogen) for immunofluorescence and goat anti-rabbit or mouse IgG coupled to IRDye800CW (LI-COR Biotechnology) for Western blotting.

Immunofluorescence staining and confocal microscopy analysis

Immunofluorescence experiments were performed as described previously [27], with minor modifications. Cells were seeded on to glass coverslips and transfected with NEU3 and with Rab5–GFP, Rab11a–GFP, β4GalNAcT-I–Cherry, LAMP1–GFP, CLC–EYFP, AP-2 σ2–GFP or PH-PLCδ1–RFP when indicated. At 24 h post-transfection, cells were analysed *in vivo* by confocal microscopy or fixed with 1 % (w/v) paraformaldehyde in PBS for 10 min. After washes with PBS, cells were incubated with primary and secondary antibodies. In some cases, cells were permeabilized with 0.1 % Triton X-100/200 mM glycine in PBS for 2 min at room temperature. Nuclei were stained blue with Hoechst 33258 dye (Molecular Probes/Invitrogen). For staining of the plasma-membrane-associated gangliosides, cells were incubated with antibody against GD3, antibody against GD1a or CTxβ (CTx β-subunit) (which binds to GM1) at 4 °C for 60 min before fixation. Confocal images were collected using an Olympus FluoView FV1000 confocal microscope equipped with an argon/helium/neon laser and a ×63 (numerical aperture 1.4) oil-immersion objective (Zeiss Plan-Apochromat). Single confocal sections of 0.8 μm were taken parallel to the coverslip

(*xy* sections). In some cases, confocal slices of 0.2 μm were taken perpendicular to the image plane (z-slices).

Image processing

Final images were compiled with Adobe Photoshop CS4, with the confocal fluorescence micrographs in the present paper being representative of at least three independent experiments. Scale bars in all Figures represent 10 μm. Quantification of fluorescence intensity (arbitrary units/cell area) of a focal plane of at least 20 cells of each experimental condition was performed using ImageJ software (NIH). Quantification of the number of clathrin, AP-2 and caveolin-1 pits of at least 20 cells of each experimental condition was performed using the Particle Analysis ImageJ plugin. Manders' co-localization coefficients were calculated using the JACoP ImageJ plugin with at least ten cells for each experimental condition being imaged on the *z*-axis (five to ten *z*-slices).

Cargo internalization assays

For internalization experiments using Tf–Alexa^{647} (Alexa Fluor® 647-conjugated human Tf) (Molecular Probes/Invitrogen), cells grown on coverslips and transfected to express NEU3 were first incubated for 60 min at 37 °C in DMEM without FBS in order to deplete serum Tf. Then, cells were incubated for 45 min at 37 °C with pre-warmed DMEM, without FBS, supplemented with 4 μg/ml Tf–Alexa^{647}. To concentrate the cargo at early endosomes [31], cells were incubated with DMEM containing 4 μg/ml Tf–Alexa^{647} at 16 °C for 30 min. To avoid endocytosis and to concentrate Tf mainly at the cell surface, cells were incubated with DMEM containing 4 μg/ml Tf–Alexa^{647} at 4 °C for 30 min. 0.6 % BSA was used in all experiments of Tf binding and uptake. After washes with cold PBS, cells were analysed in vivo by confocal microscopy or fixed and immunostained as described above. For endocytosis experiments using α_2M–Alexa^{594} (Alexa Fluor® 594-conjugated α_2M) (generously supplied by G. Chiabrando, CIBICI-CONICET, National University of Córdoba, Argentina), fluorescent LDL (BODIPY–LDL; generously supplied by C. Touz, INIMEC-CONICET, Córdoba, Argentina) and CTxβ–Alexa^{555} (Alexa Fluor® 555-conjugated CTxβ) (Molecular Probes/Invitrogen), the NEU3-expressing cells were first incubated for 60 min at 37 °C in DMEM without FBS and then with pre-warmed DMEM supplemented with α_2M–Alexa^{594} (60 nM), BODIPY–LDL (8 μg/ml) or CTxβ (0.2 μg/ml) for 30 min at 37 °C. Finally, cells were washed, fixed in 1 % (w/v) paraformaldehyde and processed for immunofluorescence and confocal microscopy.

Ganglioside and phosphoinositide depletion

To reduce GM3, GD3 and the neutral glycosphingolipid content, cells were treated with 2.4 μM P4 (D,L-threo-1-phenyl-2-hexadecanoylamino-3-pyrrolidino-1-propanol-HCl) (Matreya) [30]. After P4 treatment, cells were transfected to express NEU3 and then subjected to Tf internalization at 37 °C as indicated above. Hydrolysis of phosphoinositides was initiated by the addition of 10 μM ionomycin (Sigma–Aldrich) in the presence of 1.5 mM external calcium for 1 min at 37 °C. PtdIns(4,5)P_2 hydrolysis is reflected in the redistribution of the probe fluorescence from the plasma membrane into the cytosol [32].

Western blotting

Cell homogenates were resolved by SDS/PAGE (12 % gels) under reducing conditions. Proteins were electrophoretically transferred to nitrocellulose membranes. For immunoblotting, non-specific binding sites on the nitrocellulose membrane were blocked with 5 % (w/v) defatted dry milk powder in 400 mM NaCl and 100 mM Tris/HCl, pH 7.5. A mouse antibody against c-Myc or specific antibody against NEU3 was used. Bands of proteins were detected using an Odyssey infrared imaging system (LI-COR Biotechnology) with goat antibody against rabbit or mouse IgG coupled to IRDye800CW (LI-COR Biotechnology). Molecular masses were calculated based on calibrated standards (Spectra Multicolor Broad Range Protein Ladder; Life Technologies) run in every gel. For subcellular fractionation, cells were mechanically lysed and the homogenates were ultracentrifuged at 90 000 rev./min. NEU3 expression in both supernatant (S) and pellet (P) fractions was determined by Western blotting using an antibody against NEU3. For internalization experiments using Tf–Alexa^{647}, cells stably expressing NEU3 were first incubated for 60 min at 37 °C in DMEM without FBS in order to deplete serum Tf. Then, cells were incubated for 45 min at 37 °C with pre-warmed DMEM, without FBS, supplemented with 0.75 μg/ml Tf–Alexa^{647}. After washes with cold PBS, cells were acid stripped with 0.5 % acetic acid buffer, pH 3.5, containing 0.5 M NaCl for 5 min on ice and scrapped from the plate. Next, the homogenates were mechanically lysed and resolved by electrophoresis as described above. The Tf–Alexa^{647} transferred on to nitrocellulose membranes was detected directly taking advantage of its near-infrared fluorescence. Tubulin was used as a loading control. The images were obtained using Odyssey Application Software version 2.1, with the final images being compiled using Adobe Photoshop CS4.

Please replace 90000 rev./min. by 350000 g

RNA isolation and cDNA synthesis

Total RNA was purified using TRIzol® reagent (Invitrogen) according to the manufacturer's instructions. Total RNA (5 μg) was utilized as a template for the cDNA synthesis reaction using SuperScript™ III Reverse Transcriptase (Invitrogen) and a blend of oligo(dT) and random hexamers (Biodynamics) according to the manufacturer's instructions.

qPCR (quantitative real-time PCR)

SYBR Green-based qPCR was achieved as reported previously [33]. Primers specific to CHO-K1 endogenous *NEU1*, *NEU2* and *NEU3* were designed and purchase from Invitrogen. The quantifications were performed in Rotor-Gene Q equipment (Qiagen). The amplification mixture contained 1 μl of the cDNA synthesis reaction, 0.8 mM of each primer and 7.5 μl of Real Mix (Biodynamics) in a total volume of 15 μl. The cycling conditions were 30 s of polymerase activation at 95 °C and 40 cycles of 95 °C for 30 s, 60 °C for 30 s and 72 °C for 30 s. Each assay included a standard curve in duplicate, utilizing 1:5 serial dilutions of cDNA from CHO-K1^{GM3+} cells. Samples were measured in triplicate. The PCR product was checked by melt curve analysis, and the standard curve linearity and PCR efficiency were optimized. The data was analysed with Rotor-Gene Q software (Qiagen). The relative concentration values were normalized by the geometric average of three internal control genes: *Tbp* (TATA-box-binding protein), *GAPDH* (glyceraldehyde-3-phosphate dehydrogenase) and *18S rRNA* [34].

Metabolic labelling, lipid extraction and chromatography

Briefly, cells grown in 35-mm-diameter dishes were labelled with 30 μCi/ml [^{3}H]galactose for 24 h. After washing with ice-cold PBS, cells were scraped from the plate and pelleted by centrifugation. Lipids were extracted from the cell pellet with chloroform/methanol (2:1, v/v) and freed from water-soluble contaminants by passing through a Sephadex G-25 column. The lipid extracts and standards were chromatographed on HPTLC (high-performance TLC) plates (Merck Millipore) using chloroform/methanol/0.25 % $CaCl_2$ (60:36:8, by vol.) as solvent. Standard gangliosides were visualized by exposing the plate to iodine vapours. Radioactive gangliosides (10000 c.p.m. on each lane) were visualized by fluorography after dipping the plate in 0.4 % melted 2,5-diphenyloxazole in 2-methylnaphthalene and exposure to a radiographic film at $-70\,^{\circ}$C.

Statistical analyses

Results are presented as means$\pm$S.E.M. Statistical analyses were made using Student's *t* test or ANOVA with SigmaPlot 11.0 software. Significance (*) was attributed at the 95 % level of confidence ($P < 0.05$).

RESULTS

Expression of complex and highly sialylated gangliosides correlates with an increased internalization of Tf

First of all, we examined the endocytosis of Tf, the archetypical cargo for internalization through CME, in a panel of CHO-K1 cell lines genetically modified to express different ganglioside species [30] (Figure 1A). Wild-type CHO-K1 cells express predominantly the monosialoganglioside GM3 (CHO-K1^{GM3+}). Cells stably transfected with the cDNA encoding ST8Sia-I synthesizes mainly the disialoganglioside GD3 and to a lesser extent the trisialoganglioside GT3, but practically do not synthesize GM3 (CHO-K1^{GD3+}). On the other hand, CHO-K1 cells stably expressing the enzymes β4GalNAcT-I and β3GalT-IV mainly synthesize the a-series ganglioside GD1a and to a lesser extent GM1 (CHO-K1^{GD1a+}) (Figure 1B).

Tf internalization in these cells was investigated at 37 °C for 45 min as described in the Experimental section. Confocal microscopy analysis revealed a variable Tf cellular endocytosis, which was positively correlated with the degree of ganglioside complexity and sialylation level (GM3<GD3<GD1a) (Figure 1C). It is worthy of mention that under the experiential conditions used in this assay, Tf is internalized by cells and is mainly accumulated in recycling endosomes. Thus these results suggest the participation of gangliosides in the endocytic process of Tf.

Characterization of ectopically expressed human NEU3

To investigate the participation of gangliosides in the endocytosis of Tf, and taking into account the positive correlation between the degree of ganglioside sialylation and Tf endocytosis, we decided to study the consequences of ganglioside desialylation in the endocytic process by expression of the sialidase NEU3. First, we performed a detailed biochemical and cellular characterization of ectopically expressed full-length human NEU3 tagged at the C-terminal with the c-Myc epitope. Extracts from NEU3 transiently transfected CHO-K1^{GM3+} cells analysed by Western blotting with anti-c-Myc antibodies showed NEU3 migrating with an apparent molecular mass of ~56 kDa. A similar result was observed using a monoclonal antibody specific to human NEU3 (Figure 2A). No immunostained band was observed in extracts from non-transfected CHO-K1^{GM3+} cells. More than 98 % of the expressed sialidase was recovered in the rough particulate fraction obtained by ultracentrifugation (Figure 2B). As reported previously [35], NEU3 was mainly localized at the plasma membrane (Figure 2C). In addition, NEU3 was also found to localize in membranes from lysosomes (LAMP1$^+$), recycling endosomes (Rab11$^+$) and early endosomes (Rab5$^+$). However, NEU3 did not co-localize with β4GalNAcT-I, a Golgi marker (Figure 2D). In all cases, the organelle markers revealed the typical morphology and intracellular distribution in CHO-K1^{GM3+} cells expressing NEU3, allowing us to discard any changes at this level being associated with the expression of the sialidase. Next, we evaluated the NEU3 enzymatic activity. Since gangliosides GD3 and GD1a can be detected with specific monoclonal antibodies, we investigated the enzymatic activity of NEU3 on GD3 and GD1a substrates in CHO-K1^{GD3+} and CHO-K1^{GD1a+} cells respectively. As shown in Figure 2(E), NEU3 expression resulted in a clear and significant decrease in the GD3 and GD1a content, with a concomitant increase in the content of the product GM1 in CHO-K1^{GD1a+} cells, whose inner sialic acid residue is not accessible for NEU3 activity. Additionally, in CHO-K1^{GD3+} cells transiently expressing NEU3 sialidase, the *ex vivo* activity was found to be 60 % higher than in mock-transfected cells using 4-MU-NeuAc (4-methylumbelliferyl-α-D-*N*-acetylneuraminic acid) as the substrate at pH 4.5 (results not shown). Taken together, results from these experiments indicate that the expressed sialidase was enzymatically active.

Plasma-membrane-bound sialidase NEU3 impairs the CME of Tf

Having fully characterized NEU3 expression, we next investigated its role in modulating endocytosis of Tf. To carry this out, cells expressing different species of gangliosides were transiently transfected to express NEU3. Interestingly, we observed by confocal microscopy analysis that the Tf uptake drastically decreased in CHO-K1^{GM3+}, CHO-K1^{GD3+} and CHO-K1^{GD1a+} cells ectopically expressing NEU3 (Figures 3A and 3B). Moreover, a similar effect on Tf endocytosis was also observed in COS-7 cells expressing human NEU3 (Supplementary Figure S1). A similar result was also obtained in CHO-K1 cell lines stably expressing human NEU3, in which Tf endocytosis was quantified using volumetric fluorescence quantification in 3D-reconstituted imaging (results not shown) and by a biochemical approach (Figure 3C). Overall, these results suggest a participation of gangliosides in the endocytic process of Tf, which was drastically affected by expression of the sialidase NEU3.

To analyse further the participation of gangliosides in the CME of Tf, CHO-K1^{GM3+} and CHO-K1^{GD3+} cells were treated with P4, which is a potent inhibitor of UGCG (UDP-Glc:ceramide glucosyltransferase) and hence of the synthesis of GlcCer (glucosylceramide) and of more complex glycosphingolipids (see Figure 1A). As shown in Figure 3(B), general depletion of glycosphingolipids in CHO-K1^{GM3+} cells did not affect Tf endocytosis, as reported previously [36], whereas the same treatment in CHO-K1^{GD3+} cells led to a 30 % reduction in Tf endocytosis. Overall, these results suggest that glycosphingolipids are not strictly necessary for CME of Tf, but they enhance the internalization of the cargo when they are more complex and have higher amounts of sialic acids. On the other hand, the drastic reduction in Tf endocytosis caused by NEU3 was still seen in glycosphingolipid-depleted cells, suggesting that NEU3 could

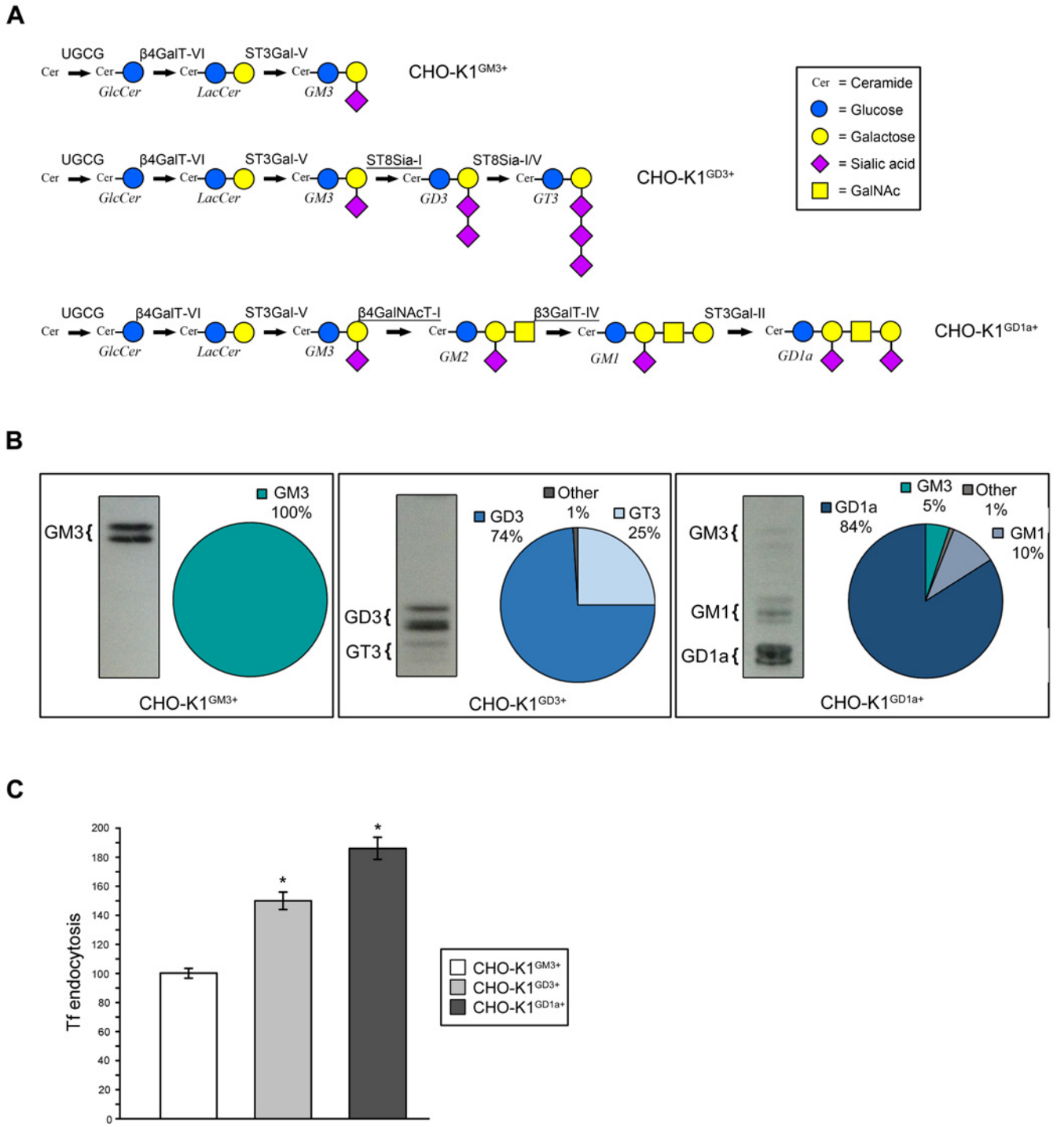

COLOUR

Figure 1 Tf endocytosis in cell lines expressing different gangliosides

(**A**) A schematic representation of ganglioside biosynthesis operating in wild-type CHO-K1 cells (CHO-K1^{GM3+}) and in CHO-K1 cell clones stably expressing ST8Sia-I (CHO-K1^{GD3+}) or β4GalNAcT-I and β3GalT-IV (CHO-K1^{GD1a+}). Glycosyltransferases that are stably expressed in each clone are underlined; the rest are endogenously expressed by wild-type CHO-K1 cells. For a description of the enzymes and glycolipids depicted, see [8,12]. (**B**) Cells were metabolically labelled with [^{3}H]galactose for 24 h. Lipid extracts were purified, chromatographed on an HPTLC plate and visualized as indicated in the Experimental section. The position of co-chromatographed radioactive ganglioside standards is indicated with brackets. Lipids migrate as multiple bands because of the heterogeneity of the fatty acyl chains in ceramide. Quantification of ganglioside content in each cell type is also shown. (**C**) Cells grown on coverslips were incubated for 45 min at 37 °C with Tf–Alexa^{647} to allow the steady-state distribution of internalized Tf. Then, cells were washed, fixed and visualized by confocal microscopy. To quantify Tf endocytosis, the whole fluorescence intensity of internalized Tf–Alexa^{647} in cells (as a percentage with respect to CHO-K1^{GM3+}) was analysed using ImageJ software.

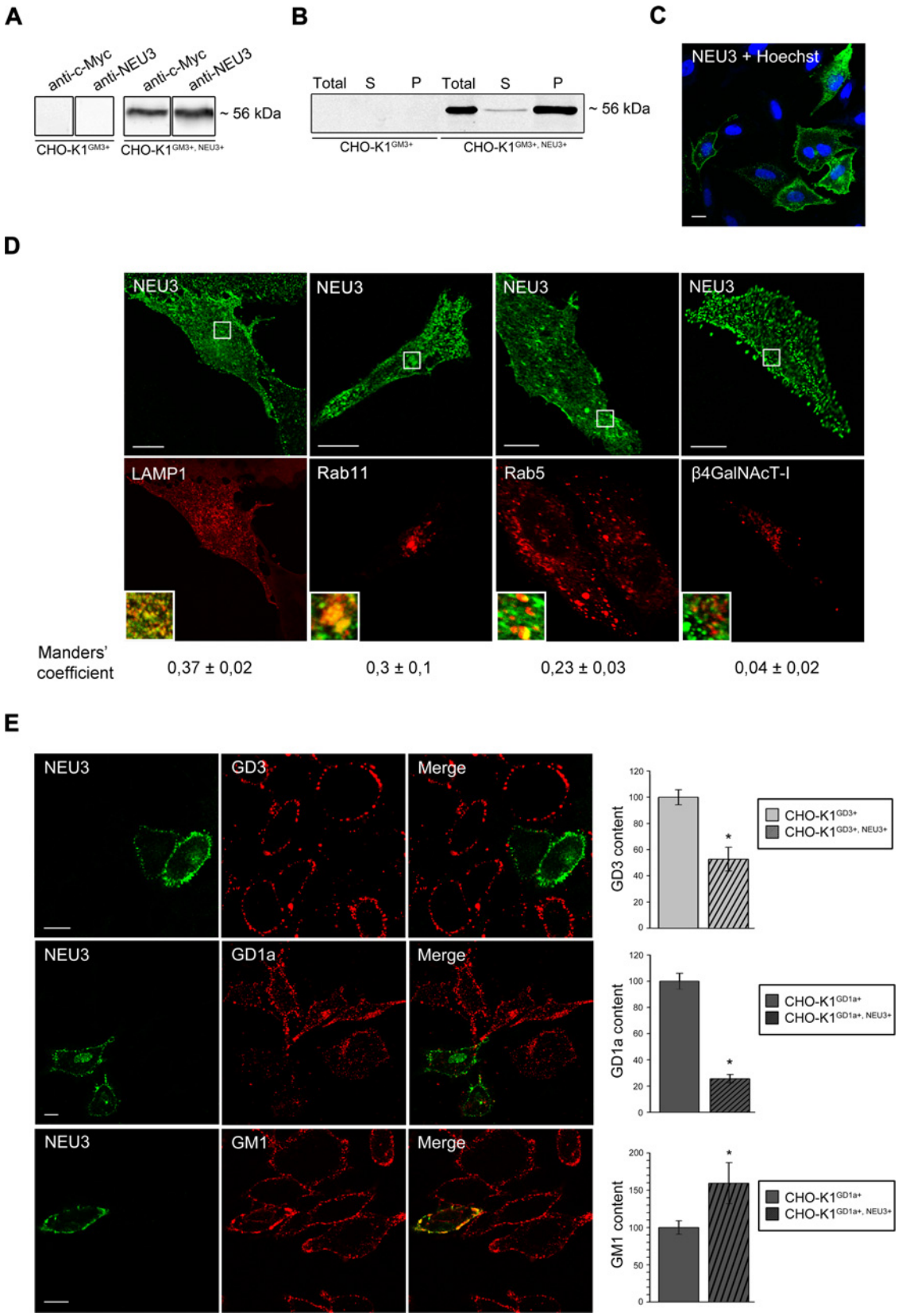

COLOUR

Figure 2 Expression and characterization of human NEU3

(**A**) Western blot of total cell homogenate of CHO-K1^{GM3+} and CHO-K1$^{GM3+,\ NEU3+}$ cells. Detection of NEU3 was carried out using anti-NEU3 or anti-c-Myc monoclonal antibodies. (**B**) CHO-K1^{GM3+} and CHO-K1$^{GM3+,\ NEU3+}$ cells were mechanically lysed, and the homogenates were ultracentrifuged. NEU3 expression in both supernatant (S) and pellet (P) fractions was determined by Western blotting using anti-NEU3 antibody. (**C**) CHO-K1$^{GM3+,\ NEU3+}$ cells were immunostained with antibody against NEU3 (shown in green) and visualized by confocal microscopy. The average efficiency

operate in a way that is probably independent of its catabolic action on gangliosides.

Tf uptake kinetics in NEU3-expressing cells

In the light of previous results, we decided to investigate further the participation of NEU3 in the endocytic process. The effect of NEU3 on Tf endocytosis was confirmed by a timelapse recording experiment in living cells. CHO-K1^{GM3+} cells were transfected with the expression vector pTracerNEU3, which expresses NEU3 and GFP under independent promoters, thereby allowing transfected cells (GFP$^+$ cells) to be detected. Tf internalization in living CHO-K1^{GM3+} cells transfected with pTracer vector (mock) was similar to that in non-transfected cells (Figure 4A, upper panels). In contrast, the ectopic expression of NEU3 induced a remarkable reduction in the kinetics of Tf uptake and its later accumulation in recycling endosomes (Figure 4A, lower panels).

Tf uptake follows the general steps of receptor-mediated endocytosis. Diferric Tf binds to the TfR (Tf receptor) on the cell surface and concentrates in clathrin-coated pits. The Tf–TfR complex is internalized via CME in an endocytic vesicle, passing through early endosomes to recycling endosomes where iron dissociates from Tf. Most of the internalized iron-free Tf–TfR complex is recycled back either from early endosomes, typically with a $t_{1/2}$ of 2–3 min, or through a slower step via the recycling endosomes, with a $t_{1/2}$ of 10–15 min [37]. Previous studies have shown that a reduction in the total number of TfR leads to a decrease in Tf internalization [38,39]. Since the first step of this process is the formation of the Tf–TfR complex, we analysed the possibility that NEU3 could be reducing TfR levels at the cell surface. Thus we measured the relative levels of Tf bound to its receptor at 4 °C to ensure that the Tf–TfR complex remained at the plasma membrane without appreciable internalization [40]. CHO-K1^{GM3+} cells expressing NEU3 were incubated with Tf–Alexa^{647} for 30 min at 4 °C, before being fixed and observed by confocal microscopy. As shown in Figure 4(B), the Tf binding at the cell surface of NEU3-expressing cells was significantly reduced. More interestingly, experiments of Tf uptake performed at 16 °C, widely used to accumulate the endocytic cargo in early endosomes, showed that NEU3 caused a notorious reduction in Tf content in this organelle (Figure 4C). These results suggest that NEU3 interferes in an early step of the endocytic process.

α_2M, LDL and CTxβ endocytosis in NEU3-expressing cells

We next investigated whether the internalization of other molecules could also have been affected by NEU3. Thus we evaluated the uptake of fluorescent α_2M, which binds to LRP1 (LDL receptor-related protein 1) and internalizes via CME [41,42] and CTxβ, which binds to ganglioside GM1 before being internalized via both clathrin-independent and -dependent pathways [43–45]. Cells transiently expressing NEU3 were incubated with DMEM supplemented with α_2M (60 nM) or CTxβ (0.2 μg/ml) for 30 min at 37 °C, before being fixed and their ligand internalization analysed by confocal microscopy. As shown in Figure 5(A), NEU3-expressing cells had a remarkable reduction in α_2M endocytosis, accounting for more than 50 % of inhibition. It was also observed that NEU3 significantly affected the internalization of LDL, which, after binding to its receptor, is internalized through CME [46] (results not shown). In contrast, the expression of NEU3 did not significantly modify the internalization of CTxβ (Figure 5B), which strongly suggests a close relationship between NEU3 activity and CME.

NEU3 affects the distribution of clathrin adaptor AP-2 complex

After clathrin, the heterotetrameric clathrin adaptor complexes are the major protein components of clathrin-coated vesicles. Many studies have shown that AP-2 (comprising α, β2, μ2 and σ2 subunits) is the predominant clathrin adaptor at the plasma membrane, whereas similar protein complexes (AP-1, AP-3 and AP-4) have been shown to localize both in endosomes and *trans*-Golgi network [3,47]. AP-2 binds clathrin, cargo and PtdIns(4,5)P_2; it interacts directly with motifs in the cytoplasmic tails of transmembrane receptors through its μ2 and σ2 subunits, and also indirectly with cargoes using its globular C-terminal appendage domains to bind accessory adaptor proteins [1,48–50]. Therefore, to explore in more detail the mechanisms by which expression of NEU3 interferes with CME, we decided to examine its effect on AP-2 and clathrin subcellular distribution. To carry this out, clones with stable expression of EYFP-tagged CLC and GFP-tagged σ2 subunit from AP-2 were generated in CHO-K1^{GM3+} cells. These clones were transfected in order to ectopically express NEU3, before being fixed, immunostained to detect NEU3 and visualized by confocal microscopy. Images displayed the expected punctate pattern of AP-2 and CLC in NEU3-negative cells (Figures 6A and 6B), which revealed clathrin-coated pits. As the expression of both fusion proteins had no effect on Tf uptake, this suggests that they did not interfere with the CME (results not shown). Interestingly, we observed that the AP-2 complex was mislocated and tended to accumulate in cells with ectopic expression of NEU3 (Figure 6A), whereas no appreciable effect on clathrin localization was observed (Figure 6B). The number of normal sized AP-2-coated pits in NEU3-expressing cells resulted significantly reduced compared with the number of pits in non-transfected cells (Figure 6A). This can be attributed to the mislocalization and the major redistribution of AP-2 into larger clusters occurring in NEU3-expressing cells, whereas the number of clathrin-coated pits was not modified by NEU3 (Figure 6B).

On the other hand, and in line with results described above, inhibition of the Tf endocytosis associated with NEU3 expression was also observed in cells from clones expressing AP-2 or CLC (results not shown). Additionally, the intracellular distribution of caveolin-1 in CHO-K1^{GM3+} cells did not reveal any appreciable changes in cells expressing NEU3 (Figure 6C). Taken together, these results suggest that the inhibitory effect of

of cell transfection was 25–35 %. Nuclei of cells were stained blue with Hoechst dye. (**D**) Subcellular localization of NEU3 by immunofluorescence. Fixed and permeabilized CHO-K1$^{GM3+, NEU3+}$ cells transiently co-expressing NEU3 and LAMP1–GFP (a lysosome marker), Rab11–GFP (a recycling endosome marker), Rab5–GFP (an early endosome marker) or β4GalNAcT-I–Cherry (a Golgi marker) were immunostained with antibody against NEU3 and visualized by confocal microscopy. Organelle markers were analysed by the intrinsic fluorescence of green and Cherry fluorescent proteins. The inset is a merge of these images showing details at a higher magnification (NEU3 pseudocoloured green and markers pseudocoloured red). Manders' coefficient (green overlapped with red) is indicated at the bottom of each image. (**E**) Analysis of NEU3 activity towards gangliosides (GD3, GD1a and GM1). Cells were incubated with antibody against GD3, antibody against GD1a or CTxβ (which binds to GM1) at 4 °C for 60 min to label the plasma-membrane-associated gangliosides. Then, cells were fixed, incubated with antibody against NEU3 and visualized by confocal microscopy. Ganglioside content was analysed by quantifying its fluorescence intensity using ImageJ software. Scale bars, 10 μm.

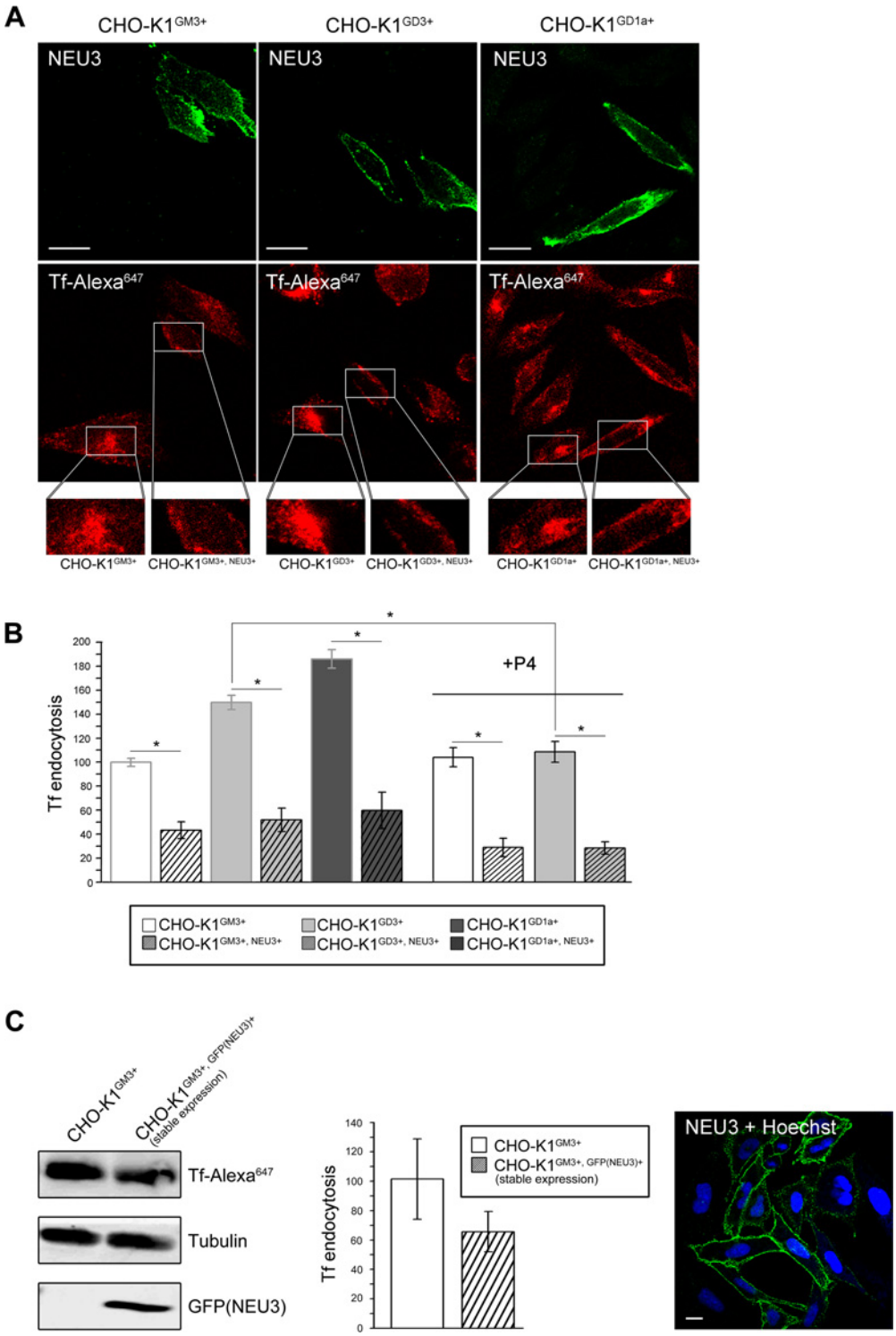

COLOUR

Figure 3 Plasma-membrane-bound sialidase NEU3 impairs the CME of Tf

(**A**) Cell lines expressing gangliosides with different levels of complexity and sialylation (CHO-K1^{GM3+}, CHO-K1^{GD3+} and CHO-K1^{GD1a+}), transiently transfected with NEU3 and grown on coverslips were incubated for 45 min at 37 °C with Tf–Alexa^{647} to allow the steady-state distribution of internalized transferrin. Then, cells were washed and fixed. Both the uptake of Tf–Alexa^{647} and the immunodetection of NEU3 were visualized by confocal microscopy. Insets show details at higher magnification of the internalized Tf in non-transfected and NEU3-transfected cells. (**B**) Tf endocytosis in cells mentioned above was analysed quantifying the whole fluorescence intensity of Tf–Alexa^{647} (as a percentage with respect to CHO-K1^{GM3+}) as indicated in the Experimental section. As a reference, Tf uptake in non-transfected cells shown in Figure 1(C) is also included (diffuse white, grey and dark grey bars). Quantification of Tf–Alexa^{647} uptake in CHO-K1^{GM3+} and CHO-K1^{GD3+} cells grown in a medium containing P4 (an inhibitor of glycosphingolipid biosynthesis) transiently transfected with NEU3. (**C**) Tf endocytosis in CHO-K1 cells stably expressing NEU3 (CHO-K1$^{GM3+,\ GFP(NEU3)+}$) analysed by Western blotting as described in the Experimental section. GFP expression was used as a marker of cells stably expressing NEU3. Tubulin was used as a loading control. Densitometric quantification of internalized Tf–Alexa^{647} and immunofluorescence of NEU3-expressing cells (NEU3 in green and Hoechst dye labelling all nuclei blue) are shown in the middle and right panels respectively. The average yield of transfection of these stable cell lines correspond to ~55–60 %. Scale bars, 10 μm.

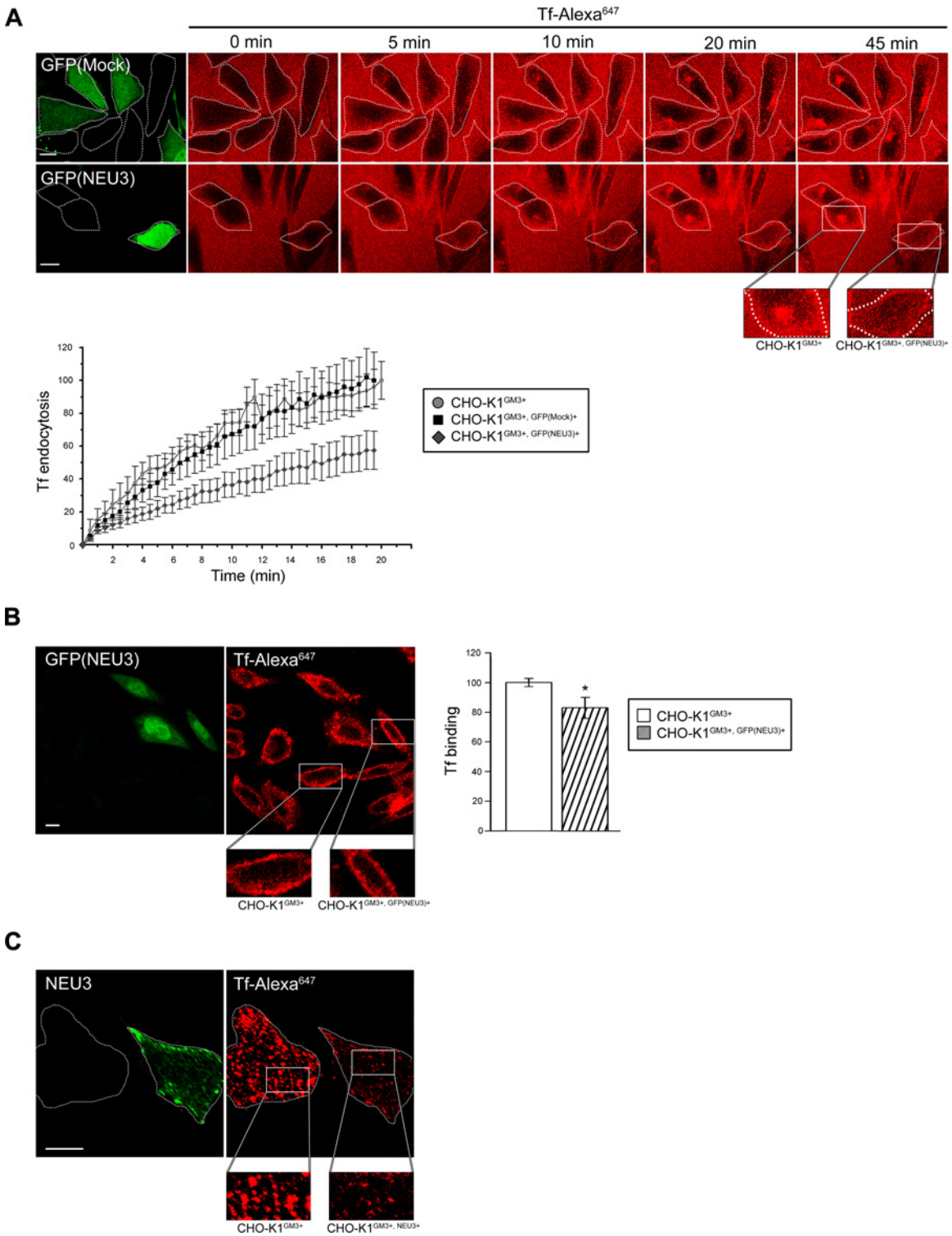

COLOUR

Figure 4 Tf uptake kinetics in NEU3-expressing cells

(**A**) Timelapse recording of Tf–Alexa^{647} uptake at 37°C in living CHO-K1^{GM3+} cells transiently transfected with pTracer vector [mock, CHO-K1$^{GM3+,GFP(Mock)+}$] or pTracerNEU3 [NEU3, CHO-K1$^{GM3+,GFP(NEU3)+}$]. The boundaries of the cells (white broken lines) are shown to facilitate discrimination between the Tf that is being endocytosed and the one that is outside the cells. Insets show details at higher magnification of the internalized Tf at 45 min in non-transfected and NEU3-transfected cells. Tf uptake kinetics were analysed by quantifying the whole fluorescence intensity of Tf–Alexa^{647} in cells (as a percentage with respect to CHO-K1^{GM3+}), using ImageJ software. (**B**) CHO-K1$^{GM3+,GFP(NEU3)+}$ cells grown on coverslips were incubated for 30 min at 4°C with Tf–Alexa^{647} to inhibit endocytic processes and to allow Tf binding at the cell surface. Then, cells were washed, fixed and visualized by confocal microscopy. Insets show details at higher magnification of Tf binding in non-transfected and NEU3-transfected cells. Tf binding was measured by quantifying the fluorescence intensity of Tf–Alexa^{647} using ImageJ software. (**C**) CHO-K1$^{GM3+,NEU3+}$ cells grown on coverslips were incubated for 30 min at 20°C with Tf–Alexa^{647} to allow Tf trafficking to early endosomes. Then, cells were washed, fixed, immunostained with antibody against NEU3 and visualized by confocal microscopy. The boundaries of the cells are shown with white broken lines. Insets show details at higher magnification. Scale bars, 10 μm.

COLOUR

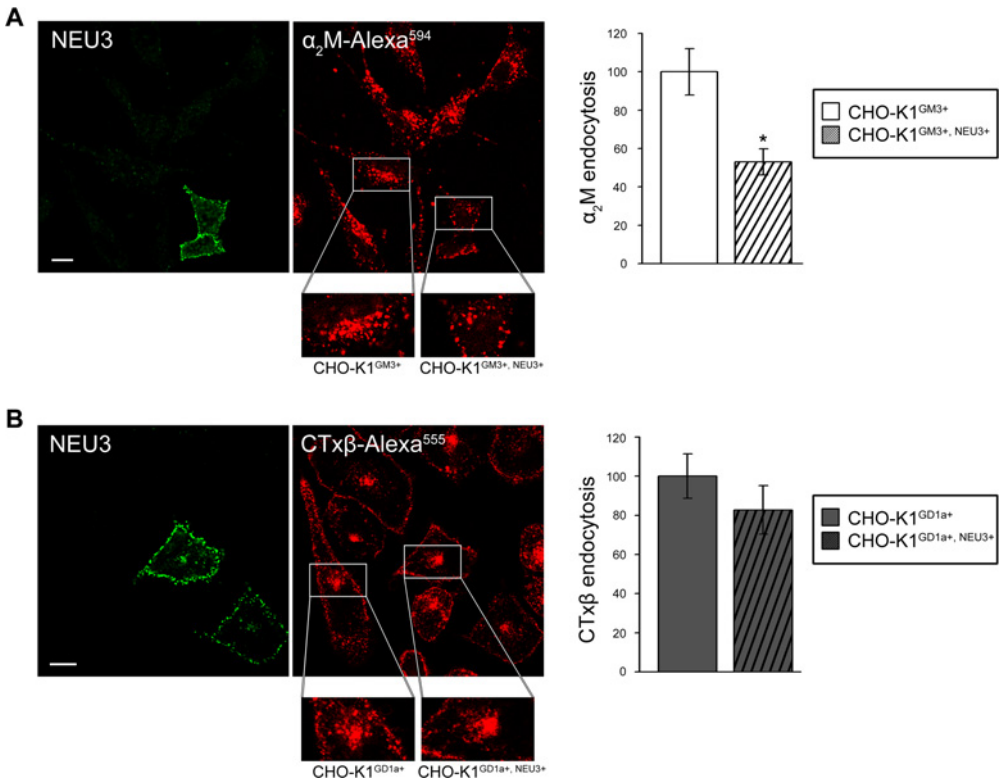

Figure 5 Endocytosis of α_2M and CTxβ

(**A**) CHO-K1$^{GM3+,\ NEU3+}$ grown on coverslips were incubated for 30 min at 37 °C with α_2M–Alexa^{594}. Then, cells were washed, fixed, immunostained with antibody against NEU3 and visualized by confocal microscopy. Insets show details at higher magnification of the internalized α_2M in non-transfected and NEU3-transfected cells. α_2M endocytosis was analysed by quantifying the whole fluorescence intensity of α_2M–Alexa^{594} in cells (as a percentage with respect to CHO-K1^{GM3+}) using ImageJ software. (**B**) CHO-K1$^{GD1a+,\ NEU3+}$ cells grown on coverslips were incubated for 30 min at 37 °C with CTxβ–Alexa^{555}. Then, cells were washed, fixed, immunostained with antibody against NEU3 and visualized by confocal microscopy. Insets show details at higher magnification of the internalized CTxβ in non-transfected and NEU3-transfected cells. CTxβ endocytosis was analysed by quantifying the whole fluorescence intensity of CTxβ–Alexa^{555} in cells (as a percentage with respect to CHO-K1^{GD1a+}) using ImageJ software. Scale bars, 10 μm.

NEU3 on CME probably occurred by affecting the functional and structural organization of coated pits, associated with an abnormal subcellular distribution of AP-2.

Effect of NEU3 expression on PtdIns(4,5)P_2 content

As mentioned above, AP-2 has binding sites for PtdIns(4,5)P_2 [48]. In addition, other accessory proteins involved in CME also contain domains that mediate their binding to PtdIns(4,5)P_2-containing membranes [i.e. epsin, dynamin or AP180 (assembly protein 180 kDa)/CALM (clathrin assembly lymphoid myeloid leukaemia protein)]. The importance of this phosphoinositide for the assembly and stability of clathrin-coated pits at the cell surface was demonstrated by targeting an inositol 5-phosphatase to the plasma membrane, which caused the dissolution of clathrin-coated pits [51]. Furthermore, up-expression of NEU3 activates the phosphoinositide 3-kinase/Akt pathway in both renal cell carcinoma and HeLa cells [52,53]. Taking all these findings into consideration, we explored whether NEU3 could exert its effect on cargo internalization by regulating PtdIns(4,5)P_2 levels at the plasma membrane. Thus CHO-K1^{GM3+} cells were transfected to co-express NEU3 and PH-PLCδ1–RFP, a PtdIns(4,5)P_2 probe. As shown in Figure 7, the expression of the sialidase did not modify the PtdIns(4,5)P_2 content or distribution at the cell surface, suggesting that the impairment of NEU3 in CME did not occur through the modulation of the cellular content of this phosphoinositide. As experimental controls, the expression of the PtdIns(4,5)P_2 probe did not modify Tf endocytosis (Figure 7A), and, as expected, the probe dissociated from the plasma membrane after treatment of cells with ionomycin, a calcium ionophore that stimulates phosphoinositides hydrolysis (Figure 7D).

DISCUSSION

In the present study, we have shown the involvement of gangliosides and sialidase NEU3 in CME. In particular, we have provided evidence that gangliosides may have a role in CME, since the complexity and sialylation level of these glycolipids correlate with an enhancement of Tf internalization (Figure 1C). Nevertheless, general depletion of glycosphingolipids in CHO-K1^{GM3+} cells had no effect on Tf internalization, whereas reduced levels of glycolipid expression in cells that normally express the disialoganglioside GD3 (CHO-K1^{GD3+}) caused a reduction of 30 % in Tf internalization. Thus these results indicate that Tf internalization can occur even in absence of glycosphingolipids, but the presence of highly sialylated gangliosides increase the amount of internalized cargo via CME.

Other major point of this work is the fact that we have provided the first evidence of the involvement of sialidase NEU3 in CME. Indeed, we found that the ectopic expression of human NEU3 led to a drastic decrease in Tf endocytosis in all cell lines used in the present study (Figure 3), further suggesting a participation of gangliosides in this process. Nevertheless, the reduction in Tf endocytosis caused by NEU3 was even

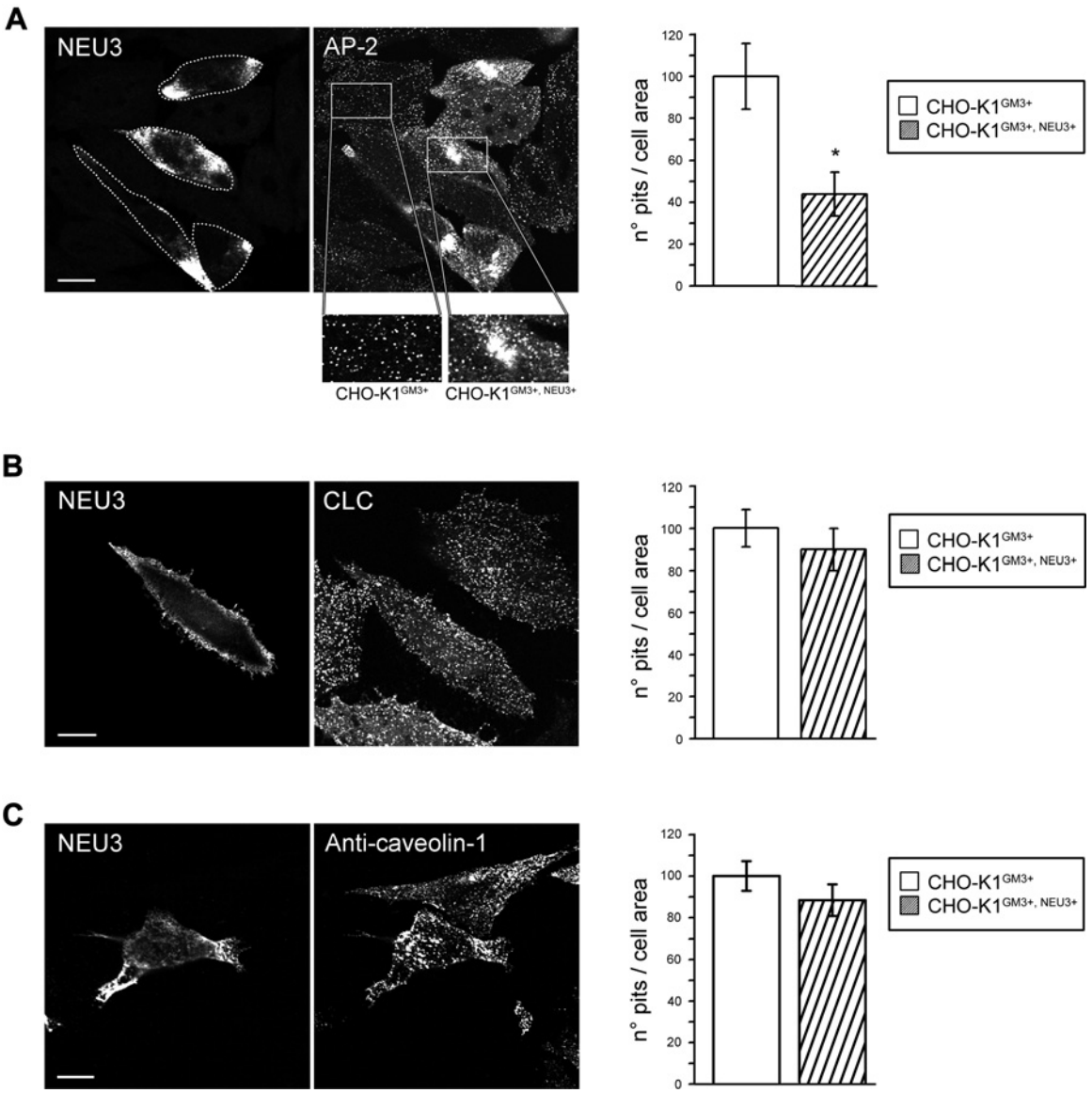

Figure 6 Effect of NEU3 on AP-2, clathrin and caveolin-1 subcellular distribution

(**A**) CHO-K1^{GM3+} cells stably expressing GFP-tagged σ2 subunit of AP-2 were transfected to transiently express NEU3, fixed, immunostained with antibody against NEU3 and analysed by confocal microscopy. Insets show details at higher magnification of AP-2 distribution in non-transfected and NEU3-transfected cells. (**B**) CHO-K1^{GM3+} cells stably expressing EYFP-tagged CLC were transfected to transiently express NEU3, fixed, immunostained with antibody against NEU3 and analysed by confocal microscopy. (**C**) CHO-K1^{GM3+} cells were transfected to transiently express NEU3, fixed, immunostained with antibody against NEU3 and endogenous caveolin-1 and visualized by confocal microscopy. Quantification of the number of AP-2, CLC or caveolin-1 pits per cell area in CHO-K1$^{GM3+,NEU3+}$ cells (as a percentage with respect to CHO-K1^{GM3+} cells) is shown in (**A**), (**B**) and (**C**) respectively. Scale bars, 10 μm.

observed in glycosphingolipid-depleted cells, indicating that NEU3 modulated CME in a way that was probably independent of its action on gangliosides. Accordingly, we can consider that NEU3 may use sialoproteins as substrates, as has been suggested previously [23,54], or, eventually, might modify the biological properties of signal molecules by physical interaction, as described previously for caveolin-1, Rac-1, Grb-2 and integrin β4 [55].

To assess whether the effect of NEU3 on CME is restricted to a specific cargo (Tf) or, in contrast, is a more general phenomenon, we evaluated the binding and internalization of α_2M and LDL molecules (other markers for CME) in cells expressing NEU3. As observed for Tf, the ectopic expression of NEU3 dramatically reduced the uptake of these ligands, whereas NEU3 expression had no appreciable effect on CTxβ endocytosis (Figure 5). Since CTxβ is endocytosed by both clathrin-dependent and -independent mechanisms, with caveolae being one of the major routes for its uptake [45,56–58], this might explain why CTxβ endocytosis remains unaltered in NEU3-expressing cells. Furthermore, cells expressing NEU3 seem to have a typical intracellular distribution of caveolin-1 (Figure 6C). Taken together, these results strongly suggest a specific and novel role for NEU3 in CME.

The effect of NEU3 on CME may be explained by a decrease in the total number of TfR at the cell surface, as demonstrated previously [38,39]. In this sense, a significant reduction in Tf

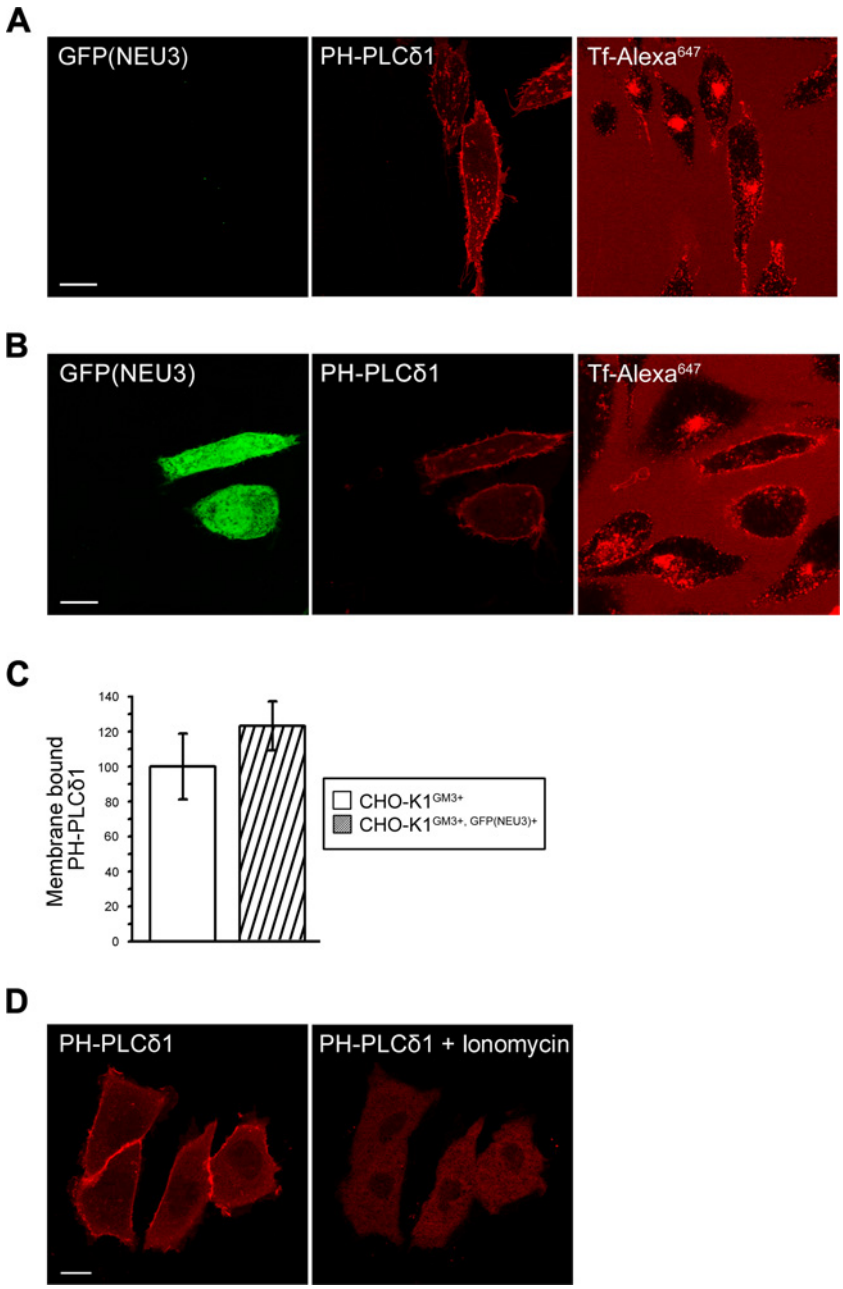

COLOUR

Figure 7 Effect of NEU3 on the cellular content and membrane distribution of PtdIns(4,5)P_2

CHO-K1^{GM3+} cells were co-transfected with pTracerNEU3 and PH-PLCδ1–RFP [a PtdIns(4,5)P_2 probe], incubated for 45 min at 37 °C with Tf–Alexa^{647} and visualized *in vivo* by confocal microscopy. (**A**) Cells single-transfected with the probe. (**B**) Cells co-transfected with both plasmids. (**C**) Membrane-bound PH-PLCδ1–RFP content in CHO-K1$^{GM3+,\ GFP(NEU3)+}$ cells with respect to CHO-K1^{GM3+} cells was analysed by quantifying the fluorescence intensity of the probe using ImageJ software. (**D**) Hydrolysis of PtdIns(4,5)P_2 was stimulated by the addition of 10 μM ionomycin in the presence of 1.5 mM external calcium for 1 min at 37 °C. PtdIns(4,5)P_2 hydrolysis is reflected in the redistribution of fluorescence from the membrane to the cytosol of PH-PLCδ1–RFP. Scale bars, 10 μm.

binding was detected at 4 °C (a well-established method for inhibiting endocytosis in mammalian cells) in NEU3-transfected cells, thus suggesting a reduction in the endogenous receptor at the plasma membrane (Figure 4B). In addition, kinetic assays carried out in cells expressing the sialidase revealed a significant reduction in the sorting of endocytosed Tf to early and recycling endosomes (Figure 4C). These findings prompted us to consider the possibility that NEU3 interferes in an early step of the endocytic process.

The formation of clathrin-coated vesicles is a complex process that involves a series of highly regulated steps. Cargo molecules, such as Tf and LDL, bind to membrane receptors having specific targeting sequences in their cytoplasmic tails, which are then involved in the recruitment to clathrin-coated pits through interaction with adaptor proteins [3,48,59]. Both clathrin and the AP-2 complex are major components of an endocytic clathrin coat with an imbalance in their functions being able to modify the normal endocytic process. In this context, previous

studies have demonstrated that AP-2 is required for efficient Tf internalization by CME [60] and that AP-2 knockdown strongly inhibits receptor-mediated endocytosis of LDL and Tf [61]. Our results show that the expression of NEU3 resulted in a remarkable subcellular redistribution of AP-2, in comparison with the normal punctate and organized structures observed at the plasma membrane of neighbouring cells that did not express the sialidase (Figure 6A). In contrast, clathrin recruitment into coated pits revealed no appreciable alteration in cells ectopically expressing NEU3 (Figure 6B). It remains to be demonstrated whether NEU3 affects directly the association of AP-2 to coated pits or results from an indirect consequence.

Phosphoinositide lipids play a central role in the organization and targeting of membrane traffic; in particular, PtdIns(4,5)P_2 is known to drive the plasma membrane localization of AP-2 [48]. Additionally, the overexpression of a mutant of epsin with a low affinity for PtdIns(4,5)P_2 was shown previously to cause AP-2 to aggregate in the cytoplasm [62]. On the basis of these findings, we decided to explore the consequences of NEU3 expression on the PtdIns(4,5)P_2 content at the cell surface. The experiments revealed that the effect of NEU3 on CME probably did not occur by modifying the cellular content or the subcellular distribution of PtdIns(4,5)P_2 (Figure 7).

Glycolipid expression results from a combination of biochemical processes, and the occurrence of cross-talk among different enzymes involved in the metabolism of these lipids has been established [13,54]. We demonstrated using qPCR that the ectopic expression of human NEU3 in CHO-K1^{GM3+} cells resulted in changes in the levels of endogenous *NEU1*, *NEU2* and *NEU3* transcripts (Supplementary Figure S2), with a similar tendency observed in the other CHO-K1 cell lines used in this work (results not shown). Consequently, this observation indicated the existence of a scenario even more complex, in which other members of the neuraminidase family should be also investigated to assess the specific role of NEU3 on CME.

In conclusion, the present study is the first demonstration of a close relationship between a sialidase of gangliosides and CME. The displacement of the AP-2 complex produced by NEU3 expression, apparently independent of its catalytic activity on gangliosides, suggests a critical role for this adaptor protein in the reduction in cargo molecule endocytosis via clathrin-coated vesicles. Nevertheless, further studies are still needed to elucidate all of the factors that induce redistribution of AP-2 and to determine the role of NEU3 in this process.

AUTHOR CONTRIBUTION

Macarena Rodriguez-Walker, Aldo Vilcaes and Eduardo Garbarino-Pico performed experiments. Macarena Rodriguez-Walker, Aldo Vilcaes and José Daniotti conceived ideas, designed experiments, analysed results and wrote the paper. All authors edited and reviewed the final paper before submission.

ACKNOWLEDGEMENTS

We thank the C. Sampedro, C. Mas, G. Schachner and S. Deza for technical assistance. We also thank Dr Paul Hobson, native speaker, for revision of the paper before submission.

(CONICET, PIP 112-20110100930)

(SECyT, 203/14)

FUNDING

Q2 This work was supported in part by grants from Secretaría de Ciencia y Tecnología (SECyT), Universidad Nacional de Córdoba (UNC), Consejo Nacional de Investigaciones Científicas y Técnicas (CONICET) and Agencia Nacional de Promoción Científica y Tecnológica (ANPCyT), Argentina. M.R-W. is a recipient of a CONICET (Argentina) fellowship. A.A.V., E.G-P. and J.L.D are career investigators of CONICET (Argentina).

(ANPCyT, PICT 2010 N° 1487, PICT 2013 N° 456)

REFERENCES

1 McMahon, H.T. and Boucrot, E. (2011) Molecular mechanism and physiological functions of clathrin-mediated endocytosis. Nat. Rev. Mol. Cell Biol. **12**, 517–533 CrossRef PubMed
2 Sigismund, S., Confalonieri, S., Ciliberto, A., Polo, S., Scita, G. and Di Fiore, P.P. (2012) Endocytosis and signaling: cell logistics shape the eukaryotic cell plan. Physiol. Rev. **92**, 273–366 CrossRef PubMed
3 Edeling, M.A., Smith, C. and Owen, D. (2006) Life of a clathrin coat: insights from clathrin and AP structures. Nat. Rev. Mol. Cell Biol. **7**, 32–44 CrossRef PubMed
4 Donaldson, J.G., Porat-Shliom, N. and Cohen, L.A. (2009) Clathrin-independent endocytosis: a unique platform for cell signaling and PM remodeling. Cell. Signal. **21**, 1–6 CrossRef PubMed
5 Hansen, C.G. and Nichols, B.J. (2009) Molecular mechanisms of clathrin-independent endocytosis. J. Cell Sci. **122**, 1713–1721 CrossRef PubMed
6 Howes, M.T., Mayor, S. and Parton, R.G. (2010) Molecules, mechanisms, and cellular roles of clathrin-independent endocytosis. Curr. Opin. Cell Biol. **22**, 519–527 CrossRef PubMed
7 Mayor, S. and Pagano, R.E. (2007) Pathways of clathrin-independent endocytosis. Nat. Rev. Mol. Cell Biol. **8**, 603–612 CrossRef PubMed
8 Daniotti, J.L. and Iglesias-Bartolome, R. (2011) Metabolic pathways and intracellular trafficking of gangliosides. IUBMB Life **63**, 513–520 CrossRef PubMed
9 Daniotti, J.L., Vilcaes, A.A., Torres Demichelis, V., Ruggiero, F.M. and Rodriguez-Walker, M. (2013) Glycosylation of glycolipids in cancer: basis for development of novel therapeutic approaches. Front. Oncol. **3**, 306 CrossRef PubMed
10 Yu, R.K., Tsai, Y.T., Ariga, T. and Yanagisawa, M. (2011) Structures, biosynthesis, and functions of gangliosides: an overview. J. Oleo Sci. **60**, 537–544 CrossRef PubMed
11 Maccioni, H.J. (2007) Glycosylation of glycolipids in the Golgi complex. J. Neurochem. **103**, 81–90 CrossRef PubMed
12 Merrill, Jr, A.H. (2011) Sphingolipid and glycosphingolipid metabolic pathways in the era of sphingolipidomics. Chem. Rev. **111**, 6387–6422 CrossRef PubMed
13 Aureli, M., Masilamani, A.P., Illuzzi, G., Loberto, N., Scandroglio, F., Prinetti, A., Chigorno, V. and Sonnino, S. (2009) Activity of plasma membrane β-galactosidase and β-glucosidase. FEBS Lett. **583**, 2469–2473 CrossRef PubMed
14 Crespo, P.M., Demichelis, V.T. and Daniotti, J.L. (2010) Neobiosynthesis of glycosphingolipids by plasma membrane-associated glycosyltransferases. J. Biol. Chem. **285**, 29179–29190 CrossRef PubMed
15 Papini, N., Anastasia, L., Tringali, C., Croci, G., Bresciani, R., Yamaguchi, K., Miyagi, T., Preti, A., Prinetti, A., Prioni, S. et al. (2004) The plasma membrane-associated sialidase MmNEU3 modifies the ganglioside pattern of adjacent cells supporting its involvement in cell-to-cell interactions. J. Biol. Chem. **279**, 16989–16995 CrossRef PubMed
16 Vilcaes, A.A., Demichelis, V.T. and Daniotti, J.L. (2011) Trans-activity of plasma membrane-associated ganglioside sialyltransferase in mammalian cells. J. Biol. Chem. **286**, 31437–31446 CrossRef PubMed
17 Anastasia, L., Papini, N., Colazzo, F., Palazzolo, G., Tringali, C., Dileo, L., Piccoli, M., Conforti, E., Sitzia, C., Monti, E. et al. (2008) NEU3 sialidase strictly modulates GM3 levels in skeletal myoblasts C2C12 thus favoring their differentiation and protecting them from apoptosis. J. Biol. Chem. **283**, 36265–36271 CrossRef PubMed
18 Sonnino, S., Aureli, M., Loberto, N., Chigorno, V. and Prinetti, A. (2010) Fine tuning of cell functions through remodeling of glycosphingolipids by plasma membrane-associated glycohydrolases. FEBS Lett. **584**, 1914–1922 CrossRef PubMed
19 Kakugawa, Y., Wada, T., Yamaguchi, K., Yamanami, H., Ouchi, K., Sato, I. and Miyagi, T. (2002) Up-regulation of plasma membrane-associated ganglioside sialidase (Neu3) in human colon cancer and its involvement in apoptosis suppression. Proc. Natl. Acad. Sci. U.S.A. **99**, 10718–10723 CrossRef PubMed
20 Mandal, C., Tringali, C., Mondal, S., Anastasia, L., Chandra, S. and Venerando, B. (2010) Down regulation of membrane-bound Neu3 constitutes a new potential marker for childhood acute lymphoblastic leukemia and induces apoptosis suppression of neoplastic cells. Int. J. Cancer **126**, 337–349 CrossRef PubMed
21 Rodriguez, J.A., Piddini, E., Hasegawa, T., Miyagi, T. and Dotti, C.G. (2001) Plasma membrane ganglioside sialidase regulates axonal growth and regeneration in hippocampal neurons in culture. J. Neurosci. **21**, 8387–8395 PubMed
22 Miyagi, T. and Yamaguchi, K. (2012) Mammalian sialidases: physiological and pathological roles in cellular functions. Glycobiology **22**, 880–896 CrossRef PubMed
23 Mozzi, A., Forcella, M., Riva, A., Difrancesco, C., Molinari, F., Martin, V., Papini, N., Bernasconi, B., Nonnis, S., Tedeschi, G. et al. (2015) NEU3 activity enhances EGFR activation without affecting EGFR expression and acts on its sialylation levels. Glycobiology, doi:10.1093/glycob/cwv026
24 Wang, Y., Yamaguchi, K., Wada, T., Hata, K., Zhao, X., Fujimoto, T. and Miyagi, T. (2002) A close association of the ganglioside-specific sialidase Neu3 with caveolin in membrane microdomains. J. Biol. Chem. **277**, 26252–26259 CrossRef PubMed

25 Tringali, C., Lupo, B., Silvestri, I., Papini, N., Anastasia, L., Tettamanti, G. and Venerando, B. (2012) The plasma membrane sialidase NEU3 regulates the malignancy of renal carcinoma cells by controlling β1 integrin internalization and recycling. J. Biol. Chem. **287**, 42835–42845 CrossRef PubMed

26 Giraudo, C.G., Rosales Fritz, V.M. and Maccioni, H.J. (1999) GA2/GM2/GD2 synthase localizes to the *trans*-Golgi network of CHO-K1 cells. Biochem. J. **342**, 633–640 CrossRef PubMed

27 Iglesias-Bartolome, R., Crespo, P.M., Gomez, G.A. and Daniotti, J.L. (2006) The antibody to GD3 ganglioside, R24, is rapidly endocytosed and recycled to the plasma membrane via the endocytic recycling compartment. Inhibitory effect of brefeldin A and monensin. FEBS J. **273**, 1744–1758 CrossRef PubMed

28 Torres Demichelis, V., Vilcaes, A.A., Iglesias-Bartolome, R., Ruggiero, F.M. and Daniotti, J.L. (2013) Targeted delivery of immunotoxin by antibody to ganglioside GD3: a novel drug delivery route for tumor cells. PLoS One **8**, e55304 CrossRef PubMed

29 Wu, X., Zhao, X., Puertollano, R., Bonifacino, J.S., Eisenberg, E. and Greene, L.E. (2003) Adaptor and clathrin exchange at the plasma membrane and *trans*-Golgi network. Mol. Biol. Cell **14**, 516–528 CrossRef PubMed

30 Crespo, P.M., Zurita, A.R. and Daniotti, J.L. (2002) Effect of gangliosides on the distribution of a glycosylphosphatidylinositol-anchored protein in plasma membrane from Chinese hamster ovary-K1 cells. J. Biol. Chem. **277**, 44731–44739 CrossRef PubMed

31 Wu, X., Zhao, X., Baylor, L., Kaushal, S., Eisenberg, E. and Greene, L.E. (2001) Clathrin exchange during clathrin-mediated endocytosis. J. Cell Biol. **155**, 291–300 CrossRef PubMed

32 Varnai, P. and Balla, T. (1998) Visualization of phosphoinositides that bind pleckstrin homology domains: calcium- and agonist-induced dynamic changes and relationship to *myo*-[^{3}H]inositol-labeled phosphoinositide pools. J. Cell Biol. **143**, 501–510 CrossRef PubMed

33 Garbarino-Pico, E., Niu, S., Rollag, M.D., Strayer, C.A., Besharse, J.C. and Green, C.B. (2007) Immediate early response of the circadian polyA ribonuclease nocturnin to two extracellular stimuli. RNA **13**, 745–755 CrossRef PubMed

34 Vandesompele, J., De Preter, K., Pattyn, F., Poppe, B., Van Roy, N., De Paepe, A. and Speleman, F. (2002) Accurate normalization of real-time quantitative RT-PCR data by geometric averaging of multiple internal control genes. Genome Biol. **3**, RESEARCH0034 CrossRef PubMed

35 Zhang, M., Koskie, K., Ross, J.S., Kayser, K.J. and Caple, M.V. (2010) Enhancing glycoprotein sialylation by targeted gene silencing in mammalian cells. Biotechnol. Bioeng. **105**, 1094–1105 PubMed

36 Cheng, Z.J., Singh, R.D., Sharma, D.K., Holicky, E.L., Hanada, K., Marks, D.L. and Pagano, R.E. (2006) Distinct mechanisms of clathrin-independent endocytosis have unique sphingolipid requirements. Mol. Biol. Cell **17**, 3197–3210 CrossRef PubMed

37 Maxfield, F.R. and McGraw, T.E. (2004) Endocytic recycling. Nat. Rev. Mol. Cell Biol. **5**, 121–132 CrossRef PubMed

38 Bourgeade, M.F., Silbermann, F., Thang, M.N. and Besancon, F. (1988) Reduction of transferrin receptor expression by interferon γ in a human cell line sensitive to its antiproliferative effect. Biochem. Biophys. Res. Commun. **153**, 897–903 CrossRef PubMed

39 Leiter, L.M., Thatte, H.S., Okafor, C., Marks, P.W., Golan, D.E. and Bridges, K.R. (1999) Chloramphenicol-induced mitochondrial dysfunction is associated with decreased transferrin receptor expression and ferritin synthesis in K562 cells and is unrelated to IRE–IRP interactions. J. Cell. Physiol. **180**, 334–344 CrossRef PubMed

40 Harding, C., Heuser, J. and Stahl, P. (1983) Receptor-mediated endocytosis of transferrin and recycling of the transferrin receptor in rat reticulocytes. J. Cell Biol. **97**, 329–339 CrossRef PubMed

41 Conner, S.D. and Schmid, S.L. (2003) Differential requirements for AP-2 in clathrin-mediated endocytosis. J. Cell Biol. **162**, 773–779 CrossRef PubMed

42 Wilsie, L.C., Gonzales, A.M. and Orlando, R.A. (2006) Syndecan-1 mediates internalization of apoE–VLDL through a low density lipoprotein receptor-related protein (LRP)-independent, non-clathrin-mediated pathway. Lipids Health Dis. **5**, 23 CrossRef PubMed

43 Chinnapen, D.J., Chinnapen, H., Saslowsky, D. and Lencer, W.I. (2007) Rafting with cholera toxin: endocytosis and trafficking from plasma membrane to ER. FEMS Microbiol. Lett. **266**, 129–137 CrossRef PubMed

44 Iglesias-Bartolome, R., Trenchi, A., Comin, R., Moyano, A.L., Nores, G.A. and Daniotti, J.L. (2009) Differential endocytic trafficking of neuropathy-associated antibodies to GM1 ganglioside and cholera toxin in epithelial and neural cells. Biochim. Biophys. Acta **1788**, 2526–2540 CrossRef PubMed

45 Torgersen, M.L., Skretting, G., van Deurs, B. and Sandvig, K. (2001) Internalization of cholera toxin by different endocytic mechanisms. J. Cell Sci. **114**, 3737–3747 PubMed

46 Marina-Garcia, N., Franchi, L., Kim, Y.G., Hu, Y., Smith, D.E., Boons, G.J. and Nunez, G. (2009) Clathrin- and dynamin-dependent endocytic pathway regulates muramyl dipeptide internalization and NOD2 activation. J. Immunol. **182**, 4321–4327 CrossRef PubMed

47 Peden, A.A., Oorschot, V., Hesser, B.A., Austin, C.D., Scheller, R.H. and Klumperman, J. (2004) Localization of the AP-3 adaptor complex defines a novel endosomal exit site for lysosomal membrane proteins. J. Cell Biol. **164**, 1065–1076 CrossRef PubMed

48 Canagarajah, B.J., Ren, X., Bonifacino, J.S. and Hurley, J.H. (2013) The clathrin adaptor complexes as a paradigm for membrane-associated allostery. Protein Sci. **22**, 517–529 CrossRef PubMed

49 Kelly, B.T., McCoy, A.J., Spate, K., Miller, S.E., Evans, P.R., Honing, S. and Owen, D.J. (2008) A structural explanation for the binding of endocytic dileucine motifs by the AP2 complex. Nature **456**, 976–979 CrossRef PubMed

50 Ungewickell, E.J. and Hinrichsen, L. (2007) Endocytosis: clathrin-mediated membrane budding. Curr. Opin. Cell Biol. **19**, 417–425 CrossRef PubMed

51 Zoncu, R., Perera, R.M., Sebastian, R., Nakatsu, F., Chen, H., Balla, T., Ayala, G., Toomre, D. and De Camilli, P.V. (2007) Loss of endocytic clathrin-coated pits upon acute depletion of phosphatidylinositol 4,5-bisphosphate. Proc. Natl. Acad. Sci. U.S.A. **104**, 3793–3798 CrossRef PubMed

52 Bonardi, D., Papini, N., Pasini, M., Dileo, L., Orizio, F., Monti, E., Caimi, L., Venerando, B. and Bresciani, R. (2014) Sialidase NEU3 dynamically associates to different membrane domains specifically modifying their ganglioside pattern and triggering Akt phosphorylation. PLoS One **9**, e99405 CrossRef PubMed

53 Ueno, S., Saito, S., Wada, T., Yamaguchi, K., Satoh, M., Arai, Y. and Miyagi, T. (2006) Plasma membrane-associated sialidase is up-regulated in renal cell carcinoma and promotes interleukin-6-induced apoptosis suppression and cell motility. J. Biol. Chem. **281**, 7756–7764 CrossRef PubMed

54 Valaperta, R., Chigorno, V., Basso, L., Prinetti, A., Bresciani, R., Preti, A., Miyagi, T. and Sonnino, S. (2006) Plasma membrane production of ceramide from ganglioside GM3 in human fibroblasts. FASEB J. **20**, 1227–1229 CrossRef PubMed

55 Miyagi, T., Wada, T. and Yamaguchi, K. (2008) Roles of plasma membrane-associated sialidase NEU3 in human cancers. Biochim. Biophys. Acta **1780**, 532–537 CrossRef PubMed

56 Cho, J.A., Chinnapen, D.J., Aamar, E., te Welscher, Y.M., Lencer, W.I. and Massol, R. (2012) Insights on the trafficking and retro-translocation of glycosphingolipid-binding bacterial toxins. Front. Cell Infect. Microbiol. **2**, 51 CrossRef PubMed

57 Kenworthy, A.K., Petranova, N. and Edidin, M. (2000) High-resolution FRET microscopy of cholera toxin B-subunit and GPI-anchored proteins in cell plasma membranes. Mol. Biol. Cell **11**, 1645–1655 CrossRef PubMed

58 Montesano, R., Roth, J., Robert, A. and Orci, L. (1982) Non-coated membrane invaginations are involved in binding and internalization of cholera and tetanus toxins. Nature **296**, 651–653 CrossRef PubMed

59 Bonifacino, J.S. and Traub, L.M. (2003) Signals for sorting of transmembrane proteins to endosomes and lysosomes. Annu. Rev. Biochem. **72**, 395–447 CrossRef PubMed

60 Motley, A., Bright, N.A., Seaman, M.N. and Robinson, M.S. (2003) Clathrin-mediated endocytosis in AP-2-depleted cells. J. Cell Biol. **162**, 909–918 CrossRef PubMed

61 Boucrot, E., Saffarian, S., Zhang, R. and Kirchhausen, T. (2010) Roles of AP-2 in clathrin-mediated endocytosis. PLoS One **5**, e10597 CrossRef PubMed

62 Ford, M.G., Mills, I.G., Peter, B.J., Vallis, Y., Praefcke, G.J., Evans, P.R. and McMahon, H.T. (2002) Curvature of clathrin-coated pits driven by epsin. Nature **419**, 361–366 CrossRef PubMed

Received 18 December 2014/28 May 2015; accepted 24 June 2015
Published as BJ Immediate Publication 24 June 2015, doi:10.1042/BJ20141550